Anais XIV Simpósio Brasileiro de Sensoriamento Remoto, Natal, Brasil, 25-30 abril 2009, INPE, p. 7353-7360.

Stochastic distances and hypothesis testing in speckled data

Abraão David Costa do Nascimento[1]
Renato José Cintra[1,2]
Alejandro César Frery[3]

[1]Departamento de Estatística, Universidade Federal de Pernambuco
Cidade Universitária, 50740-540 Recife – PE, Brasil
abraao.susej@gmail.com, rjdsc@de.ufpe.br

[2]Department of Electrical and Computer Engineering, University of Calgary, Canada,
cintra@ucalgary.ca

[3]CPMAT & LCCV / Instituto de Computação, Universidade Federal de Alagoas
BR 104 Norte km 97, 57072-970 Maceió – AL, Brasil
acfrery@pq.cnpq.br

Abstract. Images obtained with coherent illumination, as is the case of sonar, ultrasound-B, laser and Synthetic Aperture Radar – SAR, are affected by speckle noise which reduces the ability to extract information from the data. Specialized techniques are required to deal with such imagery, which has been modeled by the $\mathcal{G}^0$ distribution and under which regions with different degrees of roughness and mean brightness can be characterized by two parameters; a third parameter, the number of looks, is related to the overall signal-to-noise ratio. Assessing distances between samples is an important step in image analysis; they provide grounds of the separability and, therefore, of the performance of classification procedures. This work derives and compares eight stochastic distances and assesses the performance of hypothesis tests that employ them and maximum likelihood estimation. We conclude that tests based on the triangular distance have the the closest empirical size to the theoretical one, while those based on the arithmetic-geometric distances have the best power. Since the power of tests based on the triangular distance is close to optimum, we conclude that the safest choice is using this distance for hypothesis testing, even when compared with classical distances as Kullback-Leibler and Battacharyya.

Keywords: information theory, SAR imagery, contrast measures teoria da informação, imagens SAR, medidas de contraste.

1. Introduction

The operation of Synthetic Aperture Radar (SAR) consists of sending electromagnetic pulses towards a target and analyzing the returning echo, whose intensity depends on the physical properties of the target surface (OLIVER; QUEGAN, 1998).

Noise is inherent to image acquisition. An important source of noise when coherent illumination is used is due to the interference of the signal backscattering by the elements of the target surface. The resulting effect is called speckle noise (OLIVER; QUEGAN, 1998).

Modelling the probability distribution of image regions can be a venue for image analysis (CONRADSEN et al., 2003). In particular, the widely employed multiplicative model leads to the suggestion of the $\mathcal{G}^0$ distribution for data obtained from coherent illumination systems (FRERY et al., 1997; MEJAIL et al., 2001).

A direct statistical approach leads to the use of estimated parameters for data analysis, but a single scalar measure would be more useful when dealing with images. Such measure can be refereed to as "contrast". Suitable measures of contrast not only provide useful information about the image scene but also take part of pre-processing steps in several image analysis procedures as, for instance, image indexing (SCHOU et al., 2003).

Recent years have seen an increasing interest in adapting information-theoretic tools to image processing (GOUDAIL; RÉFRÉGIER, 2004). In particular, the concept of stochastic divergence (LIESE; VAJDA, 2006) has found applications in, among other areas, cluster analysis (MAK; BARNARD, 1996) and image classification (PUIG; GARCIA, 2003).

The aim of this study is to advance the analysis of contrast identification in single channel speckled data. To accomplish this goal, measures of contrast for $\mathcal{G}^0$ distributed data are proposed and assessed for intensity format. These measures are based on information theoretic divergences, and we identify the one that best separates different types of targets.

2. The $\mathcal{G}^0$ distribution for speckled data

Unlike many classes of noise found in optical imaging, speckle noise is neither Gaussian nor additive (OLIVER; QUEGAN, 1998). Proposed in the context of optical statistics, the most successful approach for speckle data analysis is the multiplicative model, which emerges from the physics of the image formation (GOODMAN, 1985).

Such model assumes that each picture element is the outcome of a random variable Z called *return*, which is the product of two independent random variables, X and Y. While the random variable X models the terrain *backscatter*, the random variable Y models the *speckle noise*.

Backscatter carries all the relevant information from the mapped area; it depends on target physical properties as, for instance, moisture and relief. A suitable distribution for the backscatter is the *reciprocal gamma* law (FRERY et al., 1997), $X \sim \Gamma^{-1}(\alpha, \gamma)$, whose density function is given by

$$f_X(x; \alpha, \gamma) = \frac{\gamma^{-\alpha}}{\Gamma(-\alpha)} x^{\alpha-1} \exp\left(-\frac{\gamma}{x}\right), \quad -\alpha, \gamma, x > 0. \tag{1}$$

Speckle Y can be described by the gamma distribution, $Y \sim \Gamma(L, L)$, with density given by

$$f_Y(y; L) = \frac{L^L}{\Gamma(L)} y^{L-1} \exp(-Ly), \quad y > 0, L \geq 1, \tag{2}$$

where the number of looks L is assumed known and constant over the whole image (ULABY; MOORE; FUNG, 1986).

Considering the distributions characterized by densities (1) and (2), and that the related

random variables are independent, the distribution associated to $Z = XY$ is given by

$$f_Z(z;\alpha,\gamma,L) = \frac{L^L\Gamma(L-\alpha)}{\gamma^\alpha\Gamma(-\alpha)\Gamma(L)} z^{L-1}\left(\gamma + Lz\right)^{\alpha-L}, \quad -\alpha,\gamma,z>0, L\geq 1. \tag{3}$$

We indicate this situation as $Z \sim \mathcal{G}^0(\alpha,\gamma,L)$. The rth moment of Z is expressed by

$$\mathrm{E}[Z^r] = \left(\frac{\gamma}{L}\right)^r \frac{\Gamma(-\alpha-r)}{\Gamma(-\alpha)}\frac{\Gamma(L+r)}{\Gamma(L)}, \tag{4}$$

if $-r/2 > \alpha$ and infinite otherwise. The homogeneity of the region depends on the choice of α, while γ controls the brightness.

Several methods for estimating parameters α and γ are available, including bias-reduced procedures (CRIBARI-NETO; FRERY; SILVA, 2002; SILVA; CRIBARI-NETO; FRERY, 2008; VASCONCELLOS; FRERY; SILVA, 2005), robust techniques (ALLENDE et al., 2006; BUSTOS; LUCINI; FRERY, 2002) and algorithms for small samples (FRERY; CRIBARI-NETO; SOUZA, 2004). In this study, because of its optimal asymptotic properties (CASELLA; BERGER, 2001), maximum likelihood estimation is employed to estimate α and γ.

Based on a random sample of size n, $\mathbf{z} = (z_1, z_2, \ldots, z_n)$, the likelihood function related to the $\mathcal{G}^0(\alpha,\gamma,L)$ distribution is given by

$$\mathcal{L}(\alpha,\gamma;\mathbf{z}) = \left(\frac{L^L\Gamma(L-\alpha)}{\gamma^\alpha\Gamma(-\alpha)\Gamma(L)}\right)^n \prod_{i=1}^{n} z_i^{L-1}(\gamma+Lz_i)^{\alpha-L}.$$

Thus, the maximum likelihood estimators for (α,γ), namely $(\widehat{\alpha},\widehat{\gamma})$, are the solution of the following system of non-linear equations:

$$\begin{cases} n\psi^0(L-\widehat{\alpha}) - n\psi^0(-\widehat{\alpha}) - n\log(\widehat{\gamma}) + \sum_{i=1}^n \log\left(\widehat{\gamma}+Lz_i\right) = 0, \\ -\frac{n\widehat{\alpha}}{\widehat{\gamma}} + (\widehat{\alpha}-L)\sum_{i=1}^n(\widehat{\gamma}+Lz_i)^{-1} = 0, \end{cases}$$

where $\psi^0(\cdot)$ is the digamma function. However, the above system of equations does not, in general, possess a closed form solution, and numerical optimization methods are considered.

3. Measures of Distance and Contrast for the $\mathcal{G}^0$ Law

Contrast analysis often addresses the problem of quantifying how distinguishable two image regions are from each other. In a sense, the need of a distance is implied. It is possible to understand an image as a set of regions that can be described by different probability laws.

Divergence measures were submitted to a systematic and comprehensive treatment in Ali e Silvey (1996), Csiszar (1967) and Salicrú et al. (1994) and, as a result, the class of (h,ϕ)-divergences was proposed.

Let X and Y be random variables defined over the same probability space, equipped with densities $f_X(x;\boldsymbol{\theta_1})$ and $f_Y(x;\boldsymbol{\theta_2})$, respectively, where $\boldsymbol{\theta_1}$ and $\boldsymbol{\theta_2}$ are parameter vectors. Assuming that both densities share a common support $I \subset \mathbb{R}$ the (h,ϕ)-divergence, between f_X and f_Y is defined by

$$D_\phi^h(X,Y) = h\left(\int_I \phi\left(\frac{f_X(x;\boldsymbol{\theta_1})}{f_Y(x;\boldsymbol{\theta_2})}\right) f_Y(x;\boldsymbol{\theta_2})\mathrm{d}x\right), \tag{5}$$

where $\phi\colon (0,\infty)\to[0,\infty)$ is a convex function, $h\colon (0,\infty)\to[0,\infty)$ is a strictly increasing function with $h(0)=0$, and indeterminate forms are assigned value zero. As presented in

Table 1, judicious choices of h and ϕ lead to some well-known divergence measures.

Table 1: (h, ϕ)-divergences and related functions ϕ and h.

(h,ϕ)-divergence	$h(y)$	$\phi(x)$
Kullback-Leibler	$y/2$	$(x-1)\log(x)$
Rényi (order β)	$\frac{1}{\beta-1}\log\left((\beta-1)y+1\right),\ 0 \leq y < \frac{1}{1-\beta}$	$\frac{x^{1-\beta}+x^{\beta}-\beta(x-1)-2}{2(\beta-1)}, 0<\beta<1$
Hellinger	$y/2, 0 \leq y < 2$	$(\sqrt{x}-1)^2$
Bhattacharyya	$-\log(-y+1), 0 \leq y < 1$	$-\sqrt{x}+\frac{x+1}{2}$
Jensen-Shannon	$y/2$	$x\log\left(\frac{2x}{x+1}\right)+\log\left(\frac{2}{x+1}\right)$
Arithmetic-geometric	y	$\left(\frac{x+1}{2}\right)\log\left(\frac{x+1}{2x}\right)+\left(\frac{x-1}{2}\right)$
Triangular	$y,\ 0 \leq y < 2$	$\frac{(x-1)^2}{x+1}$
Harmonic-mean	$-\log\left(-y/2+1\right),\ 0 \leq y < 2$	$\frac{(x-1)^2}{x+1}$

Some divergence measures lack the symmetry property required to distances, and a simple solution to have distances is to define a new measure $d_{\phi}^{h}(X,Y) = (D_{\phi}^{h}(X,Y) + D_{\phi}^{h}(Y,X))/2$, regardless whether $D_{\phi}^{h}(\cdot,\cdot)$ is symmetric or not.

When considering the distance between same distributions, only their parameters are relevant. In this case, parameter vectors $\boldsymbol{\theta_1}$ and $\boldsymbol{\theta_2}$ replace random variables symbols X and Y as the arguments of divergence and distance measures. Nascimento (2008) provides explicit expressions and numerical considerations regarding these distances for the $\mathcal{G}^0$ distribution.

Figure 1 depicts plots for the distances $d_{\phi}^{h}(\boldsymbol{\theta}_1, \boldsymbol{\theta}_2)$ between $\mathcal{G}^0$, where $\boldsymbol{\theta}_1 = (\alpha_1, \gamma_1, 8)$ and $\boldsymbol{\theta}_2 = (-12, 11, 8)$, with $\alpha_1 \in [-14, -10]$ and γ_1 was selected, using equation (4), so that its associated $\mathcal{G}^0$ distributed random variable has unit mean:

$$\gamma_1 = \frac{L\Gamma(-\alpha_1)\Gamma(L)}{\Gamma(-\alpha_1-1)\Gamma(L+1)} = -\alpha_1 - 1. \tag{6}$$

The obtained curves indicate that Hellinger and Bhattacharyya distances exhibit comparable behavior. Similarly, Kullback-Leibler, Rényi with $\beta = 0.95$, and triangular distances have closely matching plots.

Statistical hypothesis tests for the null hypothesis $\mathcal{H}_0 : \boldsymbol{\theta}_1 = \boldsymbol{\theta}_2$ can be derived from distances. In particular, the following statistic is considered:

$$S_{\phi}^{h}(\widehat{\boldsymbol{\theta}}_1, \widehat{\boldsymbol{\theta}}_2) = \frac{2mnv}{m+n} d_{\phi}^{h}(\widehat{\boldsymbol{\theta}}_1, \widehat{\boldsymbol{\theta}}_2),$$

where $v = 1/\left(h'(0)\phi''(1)\right)$ is a constant that depends on the chosen distance; see Table 2.

Proposition 1 (NASCIMENTO, 2008) *Let m and n assume large values and $S_{\phi}^{h}(\widehat{\boldsymbol{\theta}}_1, \widehat{\boldsymbol{\theta}}_2) = s$, then the null hypothesis $\boldsymbol{\theta}_1 = \boldsymbol{\theta}_2$ can be rejected at a level α if $\Pr\left(\chi_M^2 > s\right) \leq \alpha$.*

In terms of image analysis, this proposition offers a method to statistically refute the hypothesis that two samples obtained in different regions can be described by the same distribution.

4. Simulation Experiments

In order to assess the proposed contrast measures, a collection of $\mathcal{G}^0$ distributed images was generated and submitted to the statistical analysis suggested by Proposition 1. Two nominal

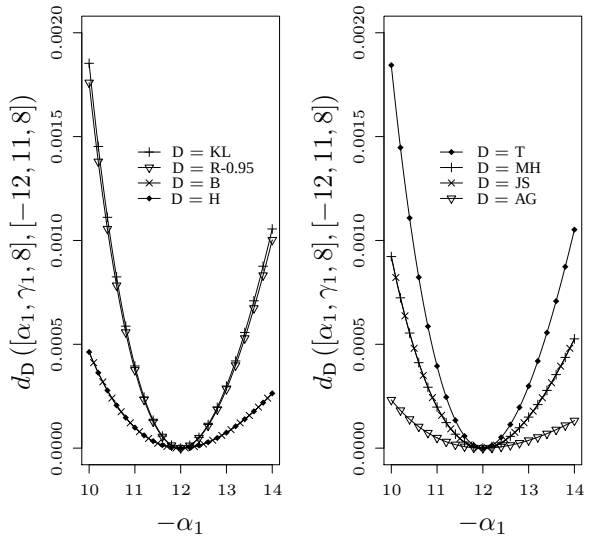

Figure 1: Distance measures between two $\mathcal{G}^0$ distributed random variables as a function of α_1.

Table 2: Distances and constants v.

Distance	v
Kullback-Leibler	1
Rényi (order β)	$1/\beta$
Hellinger	4
Bhattacharyya	4
Jensen-Shannon	4
Arithmetic-geometric	4
Triangular	1
Harmonic-mean	2

levels of significance were considered, namely 1% and 5%. We chose to worked with windows of size 7×7 pixels.

Following standard SAR literature, we index the $\mathcal{G}^0$ distribution by α and the mean $\mu = -\gamma/(1+\alpha)$.

The empirical size and power of the proposed test were sought as a means to guide the identification of the most adequate distance measure, by means of Monte Carlo experiments under four different scenarios for (α_1, μ_1, L) and (α_2, μ_2, L) and $L \in \{1, 2, 4, 8\}$: (i) $\alpha_1 = \alpha_2, \mu_1 \neq \mu_2$, (ii) $\alpha_1 \neq \alpha_2, \mu_1 = \mu_2$, (iii) $\alpha_1 < \alpha_2, \mu_1 < \mu_2$, and (iv) $\alpha_1 < \alpha_2, \mu_1 > \mu_2$. For the given selection of parameter values, pairwise combinations of the 64 image types furnished 96 different cases for each scenario (i) or (ii). Situations (iii) and (iv) offered 144 cases each.

Table 3 presents the null rejection rates of tests whose statistics S_ϕ^h are based on the discussed stochastic distances: Kullback-Leibler (S_{KL}), Rényi of order $\beta = 0.95$ (S_{R}), Hellinger (S_{H}), Bhattacharyya (S_{B}), Jensen-Shannon (S_{JS}), arithmetic-geometric (S_{AG}), triangular (S_{T}), and harmonic-mean (S_{HM}). Data was simulated obeying the null hypothesis $\mathcal{H}_0 : (\alpha_1, \gamma_1) = (\alpha_2, \gamma_2) = (\alpha^*, \gamma^*)$. Five-thousand replications were performed in each situation, but due to convergence issues in some cases lesser observations were used. The empirical rejection rates closest to the nominal level are highlighted in boldface type, and the excellent performance of

the test based on the triangular distance (S_{T}) is evident; in the few cases where it is not the best test, it is close to the optimum value.

The changes in the value of γ^* for a specific L do not alter significantly the rate of type I error. For smaller values of α^* (homogeneous images), the empirical sizes are reduced, as well as for smaller values of L. The triangular distance presents the optimum performance regarding test size. The tests yielded the empirical size closest to the theoretical one as follows: triangular in 62.50% of the 64 situations, Jensen-Shannon and harmonic-mean 9.38%, Helinger and Bhattacharyya 4.68%, Kullback-Leibler and Rényi 3.13% and, finally, arithmetic-geometric 1.57%. It is noteworthy that the two most commonly employed distances, namely the Kullbak-Leibler and the Bhattacharyya distances present poor performance when used as test statistics.

Nascimento (2008) also assesses the test power, i.e., rejection rates over several alternative hypotheses. Regarding this criterion, the test based on the triangular distance is consistently the second best, after the one derived from the arithmetic-geometric distance, but the former is still close to the theoretical value.

5. Conclusions

This paper presented eight statistical tests based on stochastic distances for contrast identification through the variation of parameters α and γ in SAR images modelled by the $\mathcal{G}^0$ distribution. The employed methodology differs from previous approaches, since it relies on the symmetrization of the (h, ϕ)-divergence obtained under the $\mathcal{G}^0$ model for intensity data.

We presented evidence suggesting that the measures S_{T}, S_{B}, S_{R}, S_{H} and S_{JS} have empirical type I errors smaller than the one based on the Kullback-Leibler distance, S_{KL}, which deserves lots of attention due to its linking with the log-likelihood function (BLATT; HERO, 2007). Regarding the power of the associated tests, the S_{AG} measure presented the best performance.

We observed that for a given number of looks, the test power performance of the proposed measures was roughly the same, suggesting the test based on the triangular contrast measure as the best tool for heterogeneity identification.

The $\mathcal{G}^0$ distribution is quite appropriate for describing situations of extreme roughness, i.e., with values of α close to zero. In this situation, despite the variability, the tests were also efficient. Furthermore, the power, in general, improves with the increase in the number of looks; that is, the measures of contrast perform better in images with better signal-to-noise ratio.

Acknowledgements

Renato J. Cintra wishes to thank the Government of Canada for supporting his tenure at the University of Calgary as a DFAIT post-doc fellow.

References

ALI, S. M.; SILVEY, S. D. A general class of coefficients of divergence of one distribution from another. *Journal of the Royal Statistical Society B*, v. 26, p. 131–142, 1996.

ALLENDE, H. et al. M-estimators with asymmetric influence functions: the GA0 distribution case. *Journal of Statistical Computation and Simulation*, v. 76, n. 11, p. 941–956, 2006.

BLATT, D.; HERO, A. O. On tests for global maximum of the log-likelihood function. *IEEE Transactions on Information Theory*, v. 53, p. 2510–2525, July 2007.

BUSTOS, O. H.; LUCINI, M. M.; FRERY, A. C. M-estimators of roughness and scale for GA0-modelled SAR imagery. *EURASIP Journal on Applied Signal Processing*, v. 2002, n. 1, p. 105–114, 2002.

CASELLA, G.; BERGER, R. L. *Statistical inference*. Belmont, CA: Duxbury Press, 2001.

CONRADSEN, K. et al. A test statistic in the complex Wishart distribution and its application to change detection in polarimetric SAR data. *IEEE Transactions on Geoscience and Remote Sensing*, v. 41, p. 4–19, 2003.

CRIBARI-NETO, F.; FRERY, A. C.; SILVA, M. F. Improved estimation of clutter properties in speckled imagery. *Computational Statistics and Data Analysis*, v. 40, n. 4, p. 801–824, 2002.

CSISZAR, I. Information type measures of difference of probability distributions and indirect observations. *Studia Scientiarum Mathematicarum Hungarica*, v. 2, p. 299–318, 1967.

FRERY, A. C.; CRIBARI-NETO, F.; SOUZA, M. O. Analysis of minute features in speckled imagery with maximum likelihood estimation. *EURASIP Journal on Applied Signal Processing*, v. 2004, n. 16, p. 2476–2491, 2004.

FRERY, A. C. et al. A model for extremely heterogeneous clutter. *IEEE Transactions on Geoscience and Remote Sensing*, v. 35, n. 3, p. 648–659, May 1997.

GOODMAN, J. W. *Statistical Optics*. New York: Wiley Series in Pure and Applied Optics, 1985.

GOUDAIL, F.; RÉFRÉGIER, P. Contrast definition for optical coherent polarimetric images. *IEEE Transactions on Pattern Analysis and Machine Intelligence*, v. 26, n. 7, p. 947–951, July 2004.

LIESE, F.; VAJDA, I. On divergences and informations in statistics and information theory. *IEEE Transactions on Information Theory*, v. 52, n. 10, p. 4394–4412, October 2006.

MAK, B.; BARNARD, E. Phone clustering using the Bhattacharyya distance. In: *The Fourth International Conference on Spoken Language Processing (ICSLP)*. Philadelphia, PA: [s.n.], 1996. v. 4, p. 2005–2008.

MEJAIL, M. E. et al. Approximation of distributions for SAR images: proposal, evaluation and practical consequences. *Latin American Applied Research*, v. 31, p. 83–92, 2001.

NASCIMENTO, A. D. C. *Contrast Measures and Stochastic Distances in a Model for Speckled Data*. Dissertação (Mestrado em Estatística) — Universidade Federal de Pernambuco, Recife, PE, 2008.

OLIVER, C.; QUEGAN, S. *Understanding synthetic aperture radar images*. Boston: Artech House, 1998.

PUIG, D.; GARCIA, M. A. Pixel classification through divergence-based integration of texture methods with conflict resolution. In: *International Conference on Image Processing (ICIP)*. Berlin: Springer, 2003. v. 3, p. 1037–1040.

SALICRÚ, M. et al. On the applications of divergence type mesures in testing statistical hypothesis. *Journal of Multivariate Analysis*, v. 51, p. 372–391, 1994.

SCHOU, J. et al. CFAR edge detector for polarimetric SAR images. *IEEE Transactions on Geoscience and Remote Sensing*, v. 41, n. 1, p. 20–32, January 2003.

SILVA, M.; CRIBARI-NETO, F.; FRERY, A. C. Improved likelihood inference for the roughness parameter of the GA0 distribution. *Environmetrics*, v. 19, n. 4, p. 347–368, 2008.

ULABY, F. T.; MOORE, R. K.; FUNG, A. K. *Microwave remote sensing active and passive: radar remote sensing and surface scattering and emission theory*. Norwood, MA: Artech House, Inc, 1986.

VASCONCELLOS, K. L. P.; FRERY, A. C.; SILVA, L. B. Improving estimation in speckled imagery. *Computational Statistics*, v. 20, n. 3, p. 503–519, 2005.

Table 3: Rejection rates of (h,ϕ)-divergence tests under $H_0\colon (\alpha_1,\gamma_1)=(\alpha_2,\gamma_2)=(\alpha^*,\gamma^*)$, $\alpha^*\in\{-1.5,-3,-5,-8\}$.

			$\alpha=1\%$								$\alpha=5\%$							
α^*	γ^*	L	S_{KL}	S_{H}	S_{T}	S_{B}	S_{JS}	S_{HM}	S_{AG}	S_{R}	S_{KL}	S_{H}	S_{T}	S_{B}	S_{JS}	S_{HM}	S_{AG}	S_{R}
-1.5	1	1	3.29	2.33	**1.58**	2.44	1.96	1.79	4.52	3.04	8.91	7.14	**5.41**	7.46	6.31	5.71	11.04	8.56
		2	4.26	3.25	**2.08**	3.55	2.75	2.45	5.87	3.98	10.60	9.20	**6.92**	9.63	8.38	7.67	11.88	10.34
		4	4.55	3.58	**2.25**	3.86	3.11	2.69	5.92	4.42	11.20	10.03	**8.15**	10.40	9.45	8.86	13.08	11.09
		8	4.80	4.13	**3.04**	4.22	3.64	3.35	6.06	4.71	11.06	10.17	**8.15**	10.44	9.26	8.68	12.45	10.90
	10	1	2.98	1.96	**1.17**	2.17	1.52	1.34	4.17	2.73	8.10	6.66	**5.05**	6.89	5.95	5.47	10.41	7.78
		2	4.28	3.15	**2.23**	3.40	2.70	2.53	5.78	4.26	11.23	9.86	**7.55**	10.12	8.79	8.05	13.22	11.08
		4	4.72	4.04	**2.67**	4.22	3.57	3.09	5.94	4.66	11.08	9.93	**7.90**	10.33	9.03	8.38	12.60	10.94
		8	5.08	4.35	**2.9**3	4.62	3.82	3.35	6.48	5.02	11.75	10.86	**8.60**	11.22	9.86	9.06	13.10	11.61
-3.0	4	1	1.82	1.29	0.78	1.41	**1.00**	0.97	2.57	1.69	**4.98**	4.33	3.64	4.45	3.92	3.73	6.55	4.89
		2	2.08	1.76	**1.18**	1.82	1.46	1.43	3.14	2.03	6.65	5.52	4.41	5.73	4.99	**4.71**	7.95	6.49
		4	3.35	2.70	**1.84**	2.90	2.35	2.07	4.46	3.15	8.80	7.82	**5.87**	8.14	6.94	6.38	10.41	8.65
		8	4.12	3.38	**2.27**	3.56	2.92	2.55	5.37	4.02	10.26	9.12	**7.27**	9.37	8.17	7.70	11.68	10.13
	40	1	2.10	1.69	**1.15**	1.69	1.40	1.43	2.93	1.88	6.08	**5.10**	4.01	5.41	4.55	4.43	7.55	5.89
		2	2.61	2.17	**1.69**	2.29	2.03	1.92	3.54	2.52	7.10	5.99	**4.90**	6.15	5.38	5.15	8.60	7.00
		4	3.41	2.75	**1.80**	2.94	2.37	2.20	4.75	3.35	9.45	8.38	**6.38**	8.63	7.51	6.81	11.53	9.28
		8	4.24	3.49	**2.34**	3.78	3.08	2.69	5.44	4.10	9.91	8.91	**6.90**	9.26	7.93	7.34	11.36	9.80
-5.0	8	1	1.79	1.33	0.83	1.52	1.15	**0.96**	2.07	1.65	**4.59**	3.99	3.03	4.18	3.67	3.44	5.92	4.50
		2	1.89	1.38	**1.13**	1.61	1.23	1.26	2.42	1.76	4.44	3.87	3.21	3.97	3.71	3.43	**5.48**	4.31
		4	2.14	1.59	**1.02**	1.80	1.34	1.21	2.82	2.00	5.93	**5.03**	3.71	5.21	4.57	4.09	7.50	5.84
		8	3.58	3.15	**2.34**	3.29	2.68	2.48	4.75	3.47	9.45	8.25	**6.34**	8.59	7.47	6.78	10.83	9.34
	80	1	1.24	**1.00**	0.76	1.05	0.86	0.76	1.76	1.19	5.09	4.52	3.71	4.80	4.18	4.23	6.61	**5.04**
		2	2.07	1.67	**1.14**	1.76	1.55	1.33	2.60	1.95	5.41	4.64	3.71	**4.92**	4.48	4.17	6.65	5.35
		4	1.99	1.49	**1.12**	1.62	1.30	1.23	2.74	1.83	6.13	5.42	4.09	5.60	**4.87**	4.37	7.38	5.97
		8	3.30	2.47	**1.71**	2.71	2.14	2.00	4.40	3.22	8.58	7.87	**6.05**	8.07	7.01	6.56	10.07	8.48
-8.0	14	1	1.32	1.19	0.86	1.25	**0.99**	1.06	1.92	1.26	3.70	2.97	2.51	3.17	2.84	2.71	**4.76**	3.50
		2	1.09	0.84	0.63	0.84	0.79	0.71	1.55	**1.04**	3.17	2.97	2.46	3.01	2.72	2.55	**4.14**	3.17
		4	1.23	1.11	0.88	1.11	1.05	**0.99**	1.69	1.23	4.35	3.68	2.86	3.86	3.33	3.10	**5.23**	4.21
		8	2.47	2.14	**1.53**	2.23	1.86	1.86	3.28	2.40	6.54	5.81	4.55	6.10	5.38	**4.92**	7.85	6.43
	140	1	1.63	1.29	0.82	1.29	1.16	**1.09**	1.84	1.56	4.08	3.47	2.79	3.60	3.26	2.99	**4.83**	3.87
		2	1.47	1.17	0.91	1.29	1.12	**1.04**	2.16	1.47	4.45	3.93	3.24	4.01	3.71	3.54	**5.22**	4.40
		4	1.89	1.78	**1.22**	1.86	1.49	1.46	2.36	1.89	**5.01**	4.40	3.85	4.63	4.08	3.99	5.88	4.95
		8	2.57	2.19	**1.55**	2.30	1.84	1.80	3.30	2.55	7.27	6.69	**5.27**	6.83	6.07	5.63	8.64	7.23